Photo Degradation in Dye-Sensitized Solar Cells

T. J. Abodunrin[1], M .L. Akinyemi[1], A. O. Boyo[2], J. A. Olugbuyiro[3]

1– Department of Physics, Covenant University Cannan land, P.M.B 1023 Ota.
2 – Department of Physics, Lagos State University, Ojo, Lagos.
3 – Department of Chemistry, Covenant University Canaan Land, P.M.B 1023 Ota.

ABSTRACT. Mesoporous TiO_2 of 20nm diameter is prepared in-tandem with organic dyes and based on Fluorine – doped SnO_2 (FTO), conducting base is produced by hydrothermal process. The prepared mesoporous Cola Acuminata (*C.acuminata*), Lupinus Arboreus (*L.arboreus*) and Bougainvillea Spectabilis (*B.spectabilis*) films (0.16 cm^2) are applied; individually and in combination as interfacial layer in-between nanocrystalline TiO_2 (NC- TiO_2) and the FTO anode in the dye-sensitized solar cell (DSSC). Absorbance index (A.I) of all three dyes was studied within wavelength range 200-900 nm for a period of 11 months, equivalent to 352 sun exposure. *C.acuminata* had A.I value 4.00 that decreased to 2.32 under exposure to AM1.5 global conditions. *B.spectabilis* A.I was 1.19 but decreased to 0.520 within same period of study. Combination of *C.acuminata* and *B.spectabilis* gave A.I value 1.40, dye cocktails of *C.acuminata*, *B.spectabilis* and *L.arboreus* gave 2.00 A.I value for same wavelength range. A UV/Vis photo spectrometer was used to determine the prominent peaks and absorbance at such wavelengths. This exponential relationship is subject of our explorative study.

Introduction. In the last decade, harvesting energy from solar insulation and direct transformation to electricity with cheap materials is a prospect many photovoltaic fabrications [1-4] depend on. Many novel ideas for efficient solar to electric conversion of energy challenge conventional p-n junction diode photovoltaics. ''Gratzel'' cells though a low –cost substitute to traditional silicon solar cells has attained only 10% yet cannot be mass produced due to practical limitations like sealing off leaking electrolytes, toxicity of certain organic solvents, desorption of dyes over time due to electrolyte used in dye-sensitized solar cells (DSSC). DSSCs are established on photoexcitation of molecules of dye grown on sintered TiO_2 mesoporous nanoparticle that traps light photons for liberating electrons from the electrolyte through the TiO_2 to a load connected to the cathode [2, 4]. Recent researches concentrate on adapting the dye for improved spectral absorbance [5], increasing stability through using conducting polymers or ionic solids instead of liquid electrolytes to improve on hole transport [4, 6] and raise to excellent condition electron transport using other possible semiconductors [7] having wide-band-gap or core-shell molecular structure [8].

An important feature in DSSC is increasing its efficiency by strategic design [9] and tailoring of TiO_2 porous structure on nanoscale level in order to increase adsorption of molecular dye thereby, quickening electron transport and electrolyte. In fabrication of our DSSC, NC-TiO_2 is deposited on transparent conducting oxide (TCO) with a thickness of 4.5×10^{-5}m and an average area of 2.8 nm. In these TiO_2 nanoparticles transferring electrons through the conduction band of TiO_2 would be ineffective as a result of electrons liberated from dye molecules having to pass through main grain boundaries before they reach TCO. Moreover, electrolyte transport is not efficient enough because of irregularity in pores generated; monitoring [10] TiO_2 nanostructures is therefore very important to increasing efficiency and current of DSSCs.

Mesoporous TiO_2 (Meso-TiO_2) is regarded a prospective choice [11] for nanoporous DSSC electrode due to its attributes; large surface area, limited grain boundaries, uniform pore structure and excellent connectivity of its mesopores. However, mesopores tend to breakdown under intense heat in the process to get a suitable crystal structure.

Generally, nanoparticles clusters [12] forming big colloidal solutions to decrease surface energy. Degussa P25 used to form NC-TiO_2 colloidal particle contains many hundred nanometers of particles in TiO_2 paste. When the screen-printing procedure is applied, it is impossible to cover the

FTO perfectly smoothly without spaces in the interface [13]. This creates a direct contact with electrolytes causing deterioration between the TCO and TiO_2 layer bringing a decrease in V_{oc} as a result of back transport of electron shown by the following expression: FTO ($2e^-$) + I_3^- FTO + $3I^-$

In our work, 3.0 nm average sized Meso-TiO_2 was formed as an interfacial layer between TiO_2 and TCO. The A.I was measured for three dye samples; *C.acuminata, B.spectabilis* and *L.arboreus* and plotted against wavelength.

Fabrication of DSSC's. Preparation of thin layer of meso-TiO_2 in cubic mesophase was formed on FTO substrate by hydrothermal process. (Degussa P25) was stirred thoroughly into conc. HNO_3 in molar ratio compositions of TiO_2 / HNO_3= 3: 5 until a smooth viscous paste was obtained. The TiO_2 paste prepared was coated on the conducting surface of FTO using screen printing method. The coated TiO_2 films were sintered to make it more compact. The produced TiO_2 film was dipped into the dye solution for adsorption at room temperature. The Pt-coated FTO used as counter electrode was prepared by heating the FTO over an open Bunsen flame moving it regularly back and forth to form a uniform layer of soot. The active area of TiO_2 film dye sensitized was 2.8 nm. The slide dimension (7.5cm X 2.5 cm X 0.5 cm) ALDRICH with resistivity 7Ω / m^2. The initial solution was aged under room temperature of 23^0C for 14 days, all deposited dye sensitized films were aged for 28 days.

Characterizations. Photocurrent-voltage measurements was obtained using a multimeter 4200 model. A 60 W Xenon lamp was used to simulate a source of light, the intensity was regulated to fit AM 1.5G one sun intensity approximately, measurements were taken indoors and also in the dark. The incident photon-to-current efficiency (IPCE) spectra was determined as a function of wavelength from 200 - 900 nm. Absorbance spectra parameters was determined by Genesys 10S V1.200 (Model 2L7J355002). The A.I coefficients for the three dyes and their mixture was determined by analysing and interpreting the spectrographs for all the samples for 11 months. The morphology of TiO_2 mesoporous films was examined using a scanning electron microscope ASPEX 3020.

Results and Discussions. Characterizations of Interfacial Meso-TiO_2. In figure d, photo-electrons network of pathway from initial nucleation on TiO_2 nanoparticles and subsequent adsorption is revealed as irregular cracks. The compact TiO_2 at the boundary of the TiO_2 particles on conductive substrates has been studied [9, 10] and a large group concluded that recombination occurs predominantly near the conductive substrate and not across the entire TiO_2 film [11]. Commercial fluorine-doped tin oxide (FTO) glass used as the TCO layer looks hazy with a rough surface appearance considerable light scattering on its surface. The formation of a uniform TiO_2 layer over the rough surface (figure 1(c- d)) of the FTO layer will therefore be difficult. In general, nanoparticles are agglomerated to form large colloids in suspensions or pastes in order to reduce the surface energy [12-14]. Although electrons move a lot in different atoms, several nanoparticle boundaries and dead-ends in a disorderly molecular structure restrict electron transport [14]. An electric field is created through a charge deposited on the surface of an oxidized wafer. This oxide will break at its weakest spot (Figure 1d), current is confined to the spot of breakdown due to surface corona charge not drifting along the top layer [15]. In the DSSCs with metal substrates, the oxidized layer is naturally formed at the interface of the TiO_2 particles on conductive substrate during thermal annealing. However, it seems that the low quality oxidized layer induced poor blocking behaviour of the DSSCs with the untreated Ti substrates. The recombination kinetics [12] were investigated by the evaluation of the rate of photo voltage decay. The HNO3-HF treatment of the Ti substrates strongly influenced the rate of the photo voltage decay. (Fig. 1 (d)). The electron recombination may lead to a lowering of the photocurrent [13], a decrease in the recombination may lead to a lowering of the photocurrent, but also to a decrease in the photo voltage by lowering the quasi-Fermi level for the electrons under illumination due to a photo voltage (decrease in photocurrent) with increasing photo voltage [14]. If the improved optical reflection at the substrate were a dominant element of enhanced performance, the V_{oc} and FF would restrictively increase and decrease respectively. An obviously possible cause for the significantly improved performance is

decreased recombination at the interface of the TiO2/conductive substrate after HNO3-HF treatment.

(a)

(b)

(c)

(d)
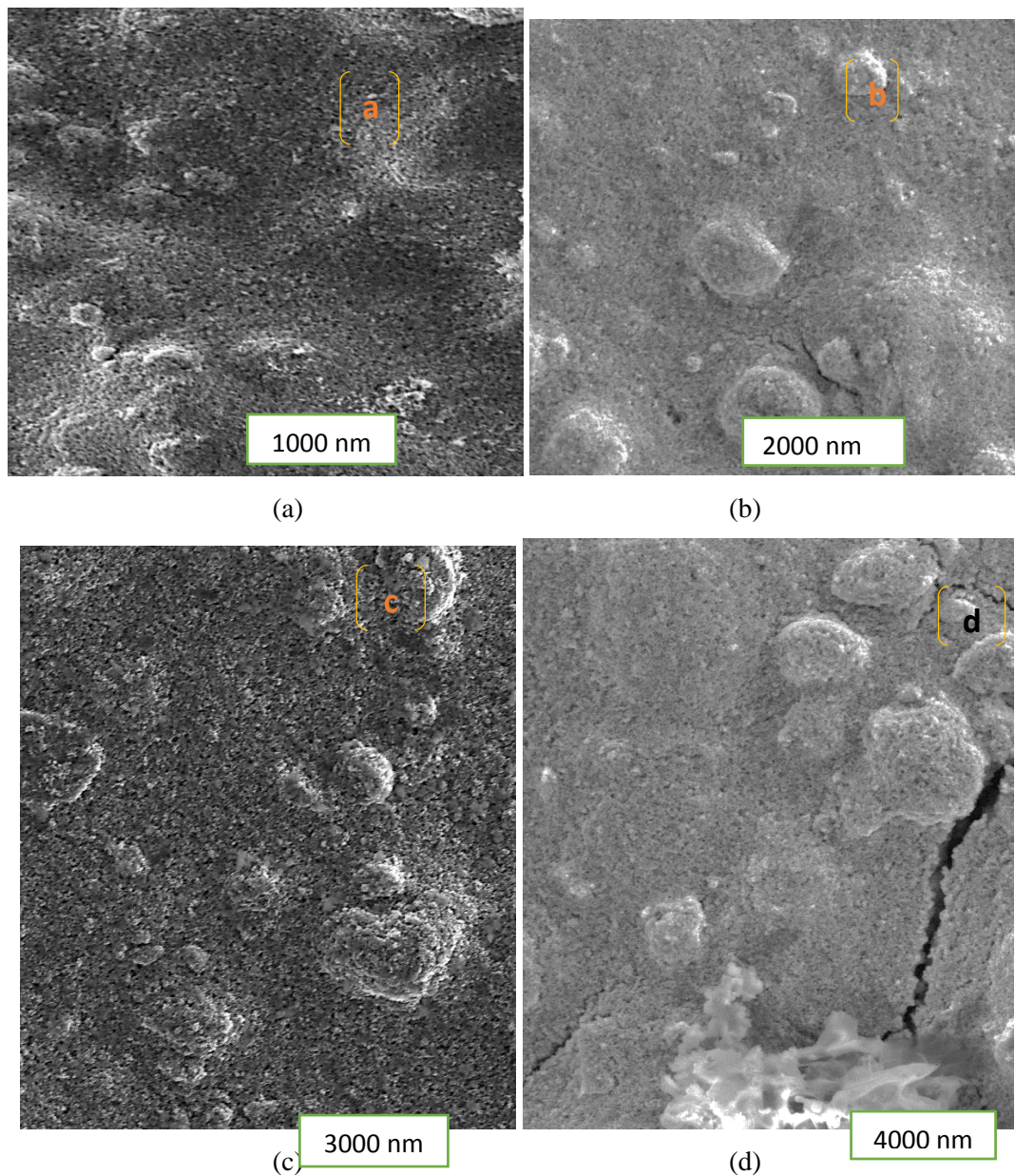
Figure 1. SEM images for Meso-TiO₂ deposited on FTO (a), (b) at different resolutions. (c) and (d) show images of nanoporous dyes articulating with meso-TiO₂ at higher resolutions.

Interactions of dyes with different electrolytes. The graphs illustrate various reactions of DSSCs with the different electrolytes; mixtute of 3:1 KBr/I, HgCl₂/I and KCl /I in sunny weather and when placed indoor. Figure 2a shows *C.acuminata* with three electrolytes, it had 5 mA, 9 mA and 3 mA with KCl, HgCl₂ and KBr respectively. KBr electrolyte did not give the desired effect; to boost the production of photocurrent. HgCl₂ increased photocurrent by 125% while, KCl's increase was 25% under AM 1.5. Figure 2a shows three intersections, where two different electrolyte record same value with dye. At this point, the physical behaviour of *C.acuminata* with KBr/I is same as *C.acuminata* with KCl/I. First intercept occurs at (3.5 mA, 1V) for KBr/I and KCl, the second is at (4.0 mA, 4V) for KBr/I and HgCl₂ in sunny weather. A third intercept is on (1.8 mA, 4V) for KBr/I and KCl/I indoors. The nanoporous *C.acuminata* dye combines with meso- TiO₂ and their reaction is same. At this point, one could be used interchangeably for the other to produce the same result.

Figure 2b reveals π to π^* transition (1 mA to 1.8 mA, 0.2V) in KCl due to the phenolic[16] bond. KBr shows series of hops (1 mA to 2 mA, 0.2V to 0.5V) before attaining a measure of stability. $HgCl_2$ experiences loss of energy due to recombination of electrons from electrolyte with holes from nanoporous dye molecules. A series of hops occur from 0.2V to 0.4V in the process of attaining stability. Figure 3a and 3b shows *B.spectabilis* outdoor and indoor respectively. An interesting observation is a combination of *B.spectabilis* with $HgCl_2$/I. Two different intersections occur at (55 mA, 30V) and (35 mA, 40V), where it is impossible to tell the behaviour and interaction of KBr/I and $HgCl_2$ with *B.spectabilis* apart, see figure 3a and 3b. Also, *B.spectabilis* indoor with $HgCl_2$/I records the same value as KBr/I which proffers a solution on days where there is little or no sunlight. In Figure 4a, an intercept occurs between KBr/I and $HgCl_2$ (2.5 mA, 10V). A π to π^* transition (4 mA to 6 mA, 12V) [16]. Figure 4b shows several 'kinks'(0.2 mA to 0.4 mA, 0.2V) for KCl/I with *L.arboreus* series of hops characteristic of electrons and holes combining with same, different holes or being trapped. Their subsequent release and recombination, which effectively reduces the effective Fermi level[17, 18] of the DSSC. Although detected by the voltmeter, because it's on nanoscale it assumes significant proportions. It affects the thermodynamic equilibrium at an electrode. An electronic circuit that is in thermodynamic equilibrium would have a constant Fermi level throughout its connected parts. A battery nor power source need not be connected[18] but, as indicated by a voltmeter. The condition is termed 'quasi-fermi' because solar illumination induced the temporary condition through a temperature difference from the sun. Also, recombination occurs (0.17 mA to 0.1 mA, 0.2 V) at the same point, π to π^* transition occur16. KBr /I with C.acuminata and B.spectabilis shows KBr/I short circuit current increase (14 mA to 17 mA, 5V) as photo electrons are generated from incident photons of sunlight. However, recombination happens (17 mA to 14 mA, 7 V), a steady state is revealed in figure 5a. This becomes short lived as short circuit current increases (13 mA to 15 mA, 18V) more photo electrons are liberated from KBr/I. Consequently, recombination happens as the hole 'moves' with the drift of electrons (15 mA to 12 mA, 20V) shown by another potential drop. Figure 5c shows an a point of intersection of HgCl2/I with KCl/I (2 mA, 15V); a juncture when C.acuminata' s cocktail with L.arboreus act alike and it is difficult to tell apart their behaviour in the two different electrolytes. In figure 5d, cocktail of B.spectabilis and L.arboreus has an intersection (2 mA, 10V) shows HgCl2/I behaving similar to KCl/I regardless of their varying chemical composition. Cocktail of C.acuminata, L.arboreus and B.spectabilis in figure 5f has an intersection (8 mA, 10V). KBr/I acts like HgCl2/I at this point which suggests that they could be used as substitutes and generate same results but, only at this point
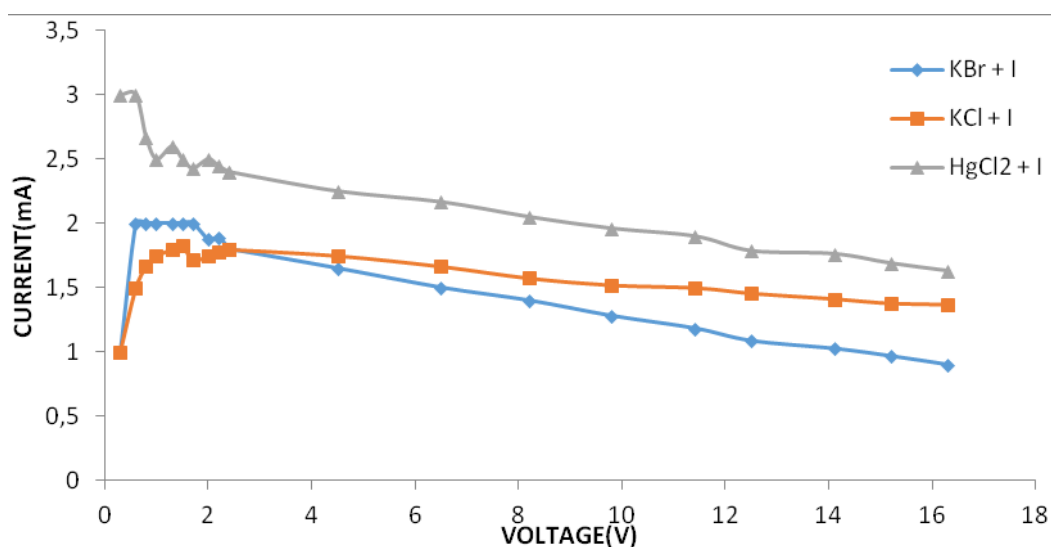
Figure 2(a). I-V curve for C.acuminata dye in Sunny weather
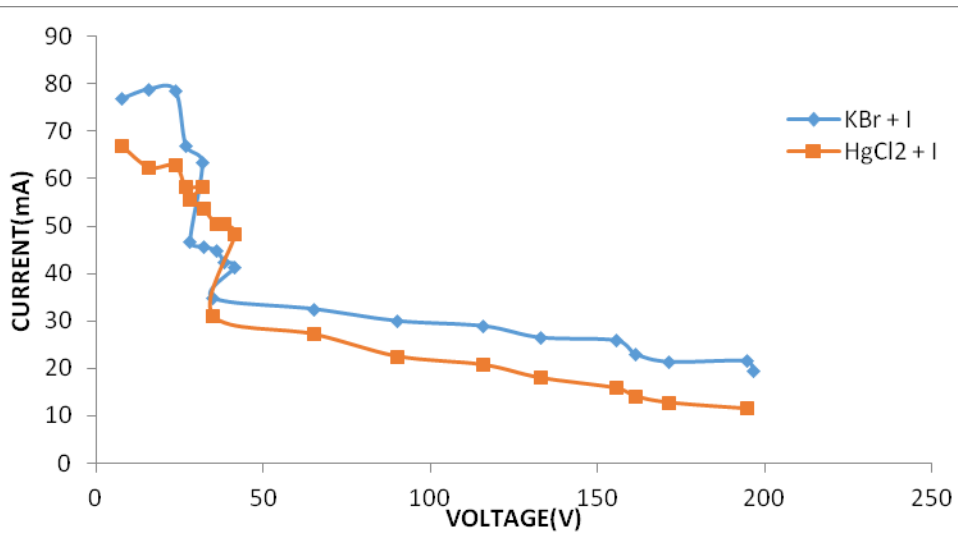
Figure 2(b). I-V curve for C.acuminata dye Indoor
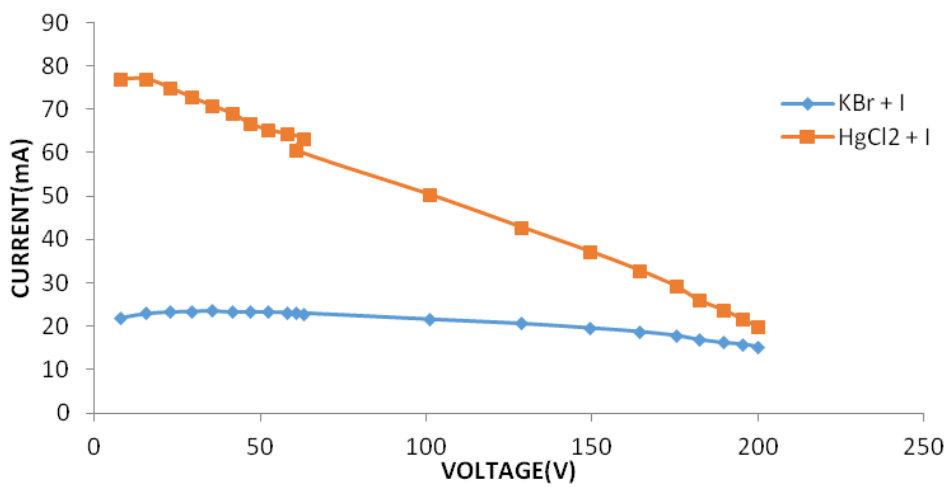
Figure 3(a). I-V curve for B.spectabilis dye in Sunny weather
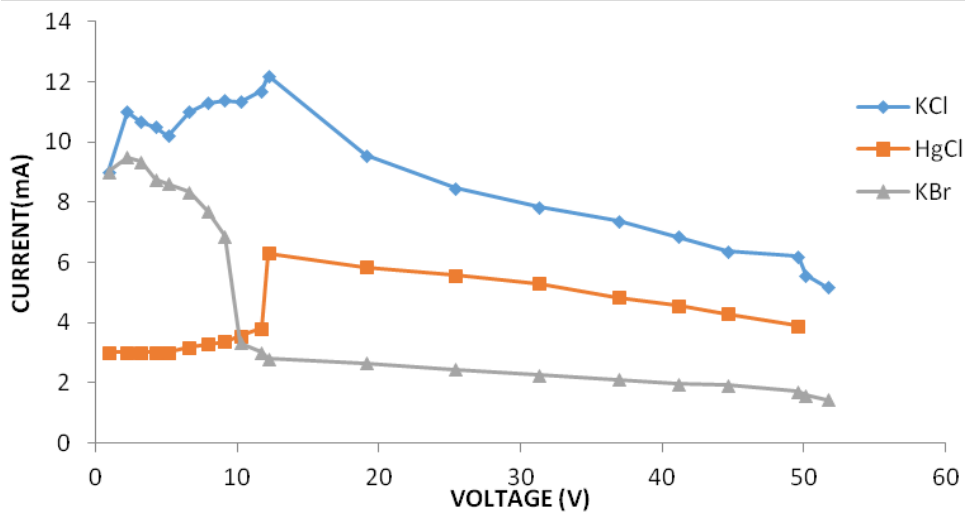
Figure 3(b). I-V curve for B.spectabilis dye Indoor
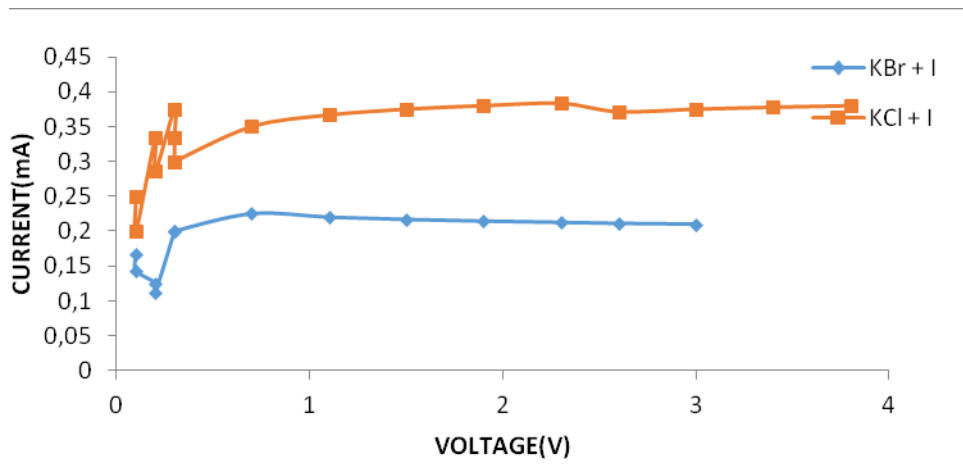
Figure 4(a). I-V curve for L.arboreus dye in Sunny weather
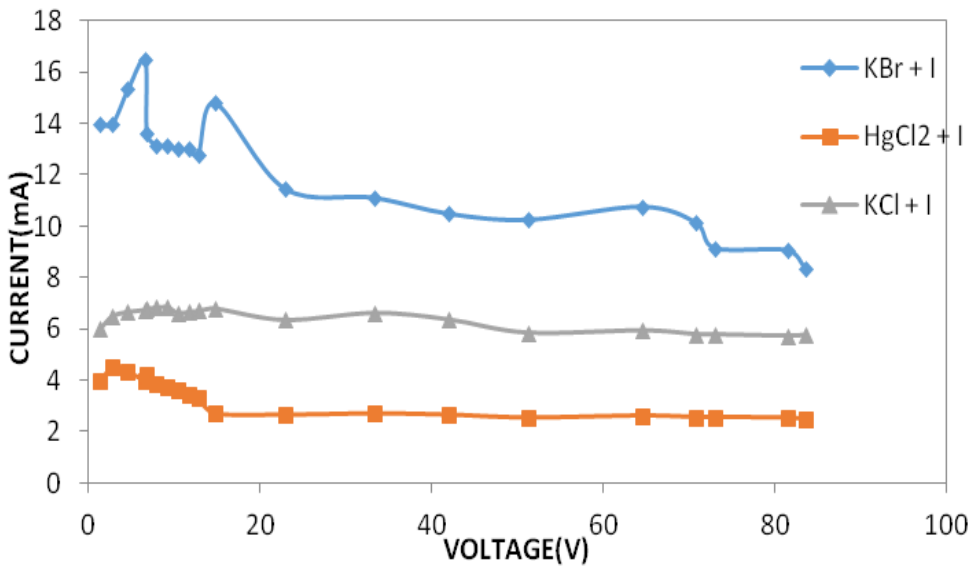
Figure 4(b). I-V curve for L.arboreus dye indoor
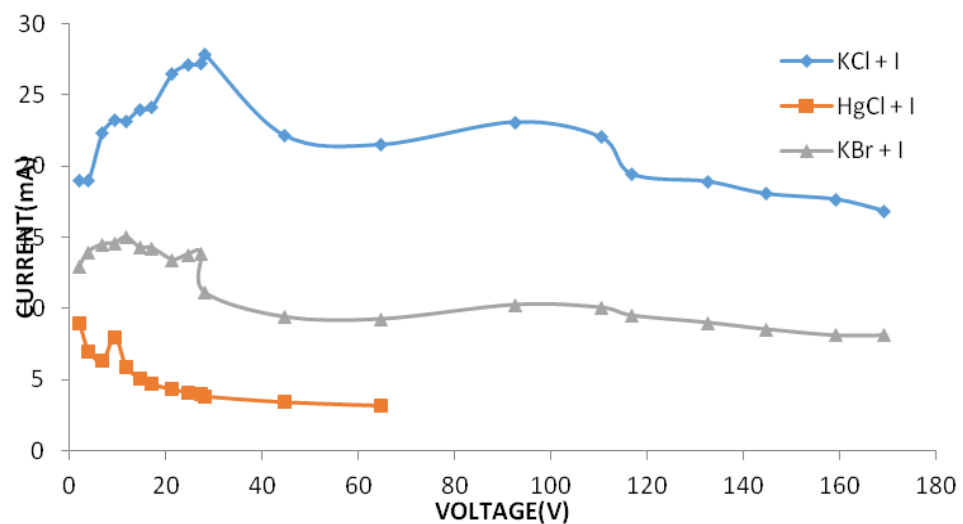
Figure 5(a). I-V curve for C.acuminata & B.spectabilis dye Indoor
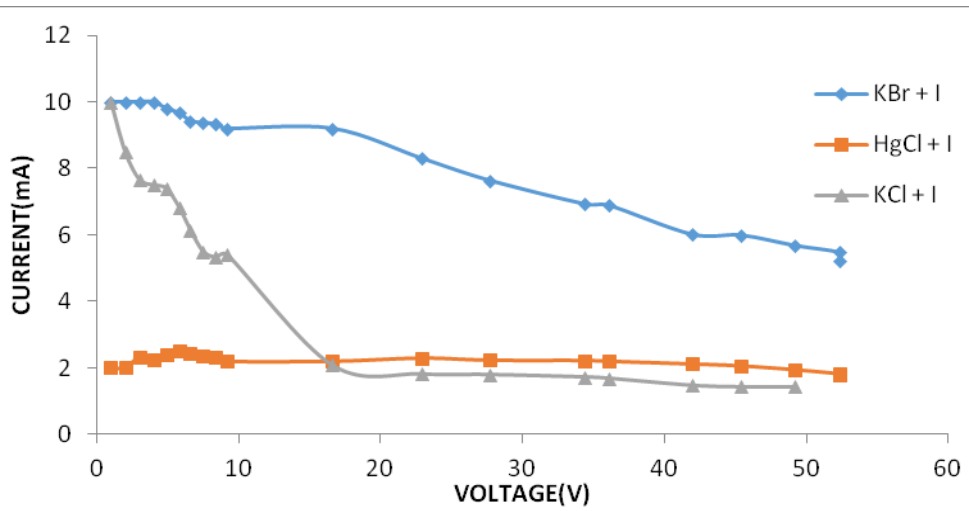
Figure 5(b). I-V curve for C.acuminata & B.spectabilis dye in Sunny weather
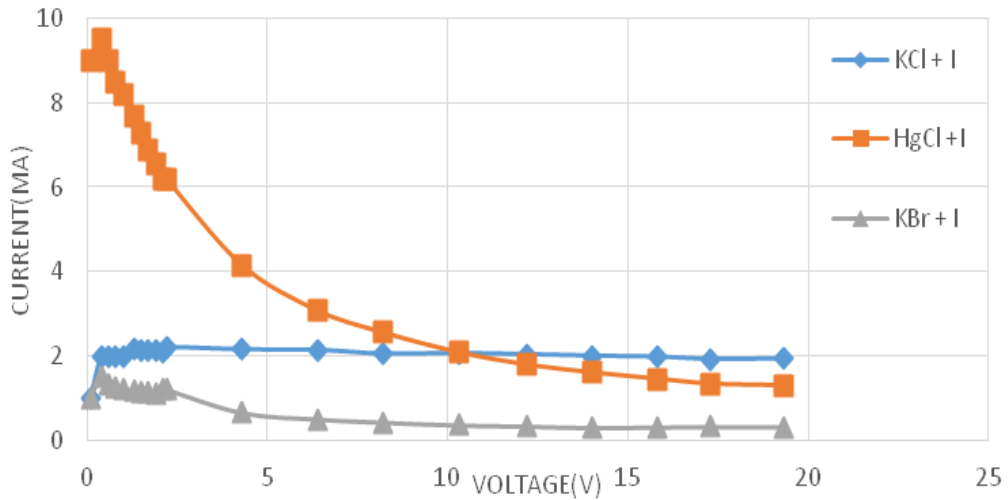
Figure 5(d). I-V curve for B.spectabilis & L.arboreus dye Indoor
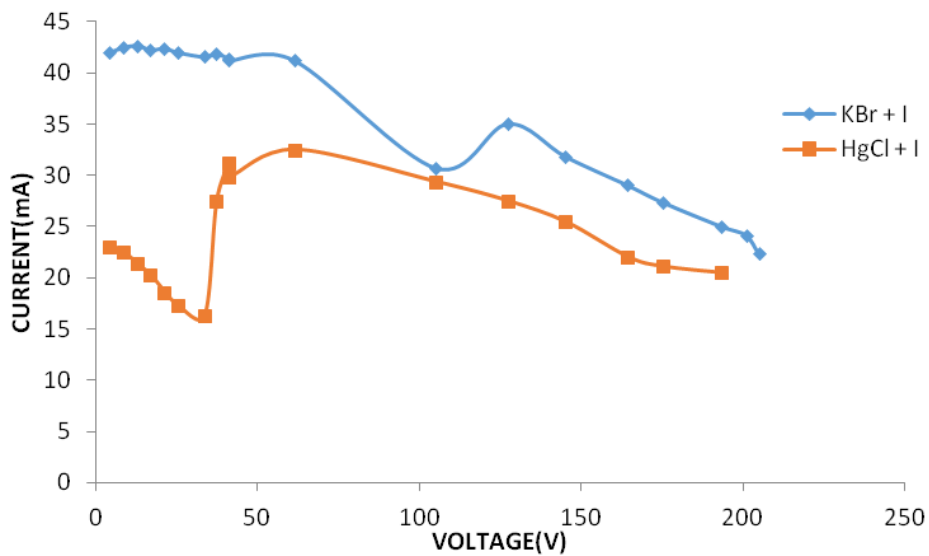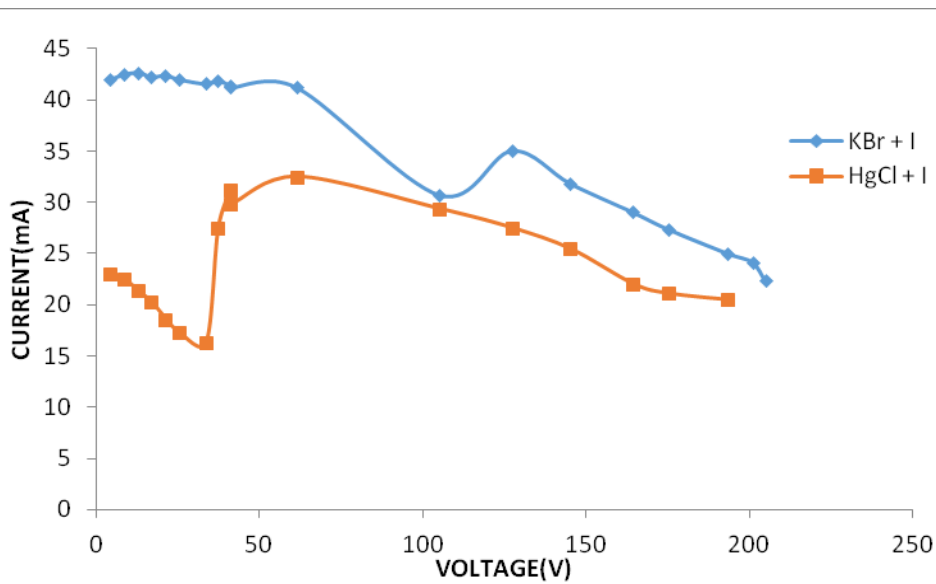
Figure 5(e). I-V curve for B.spectabilis & L.arboreus dye in Sunny weather
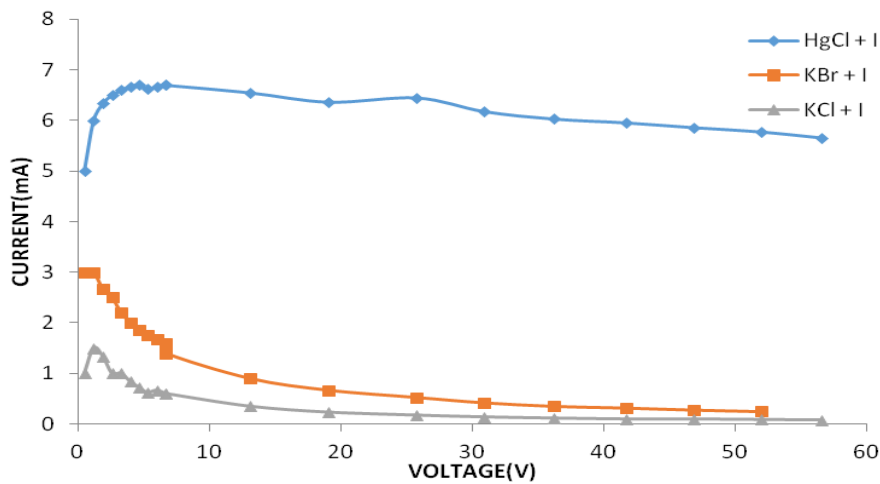
Figure 5(f). I-V curve for C.acuminata, L.arboreus & B.spectabilis dye Indoor
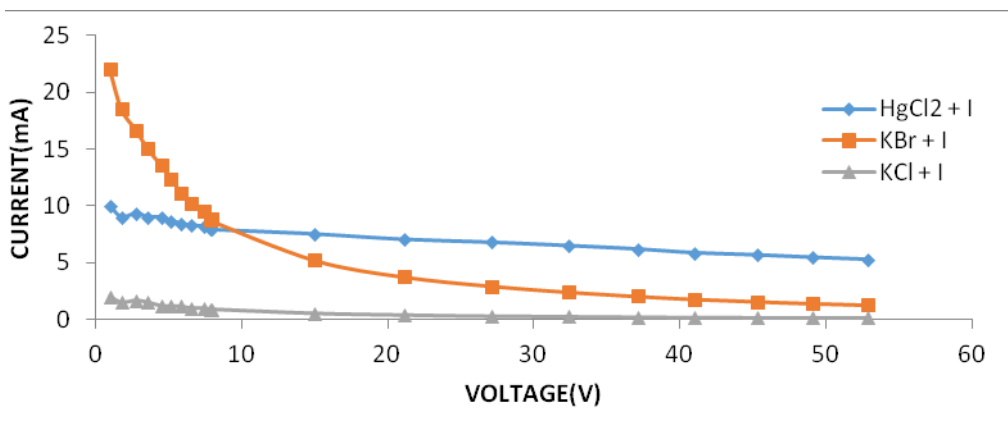
Figure 5g. I-V curve for C.acuminata, L.arboreus & B.spectabilis dye in Sunny weathe Degeneration in DSSC

Dye sensitized solar cells output efficiency decreases with age as they are exposed to ultraviolet (UV) radiation. Other obstacles are UV stabilizers that are responsible for absorbing quantized chromophores but emit only at longer wavelengths. Antioxidants used with the aim of improving cell efficiency is another hurdle that reduces the iodide ion. This iodide ion replaces the Highest

Occupied Molecular Orbital (HOMO) in the dye restoring its initial form, preparing it for generation of electron again. The reaction at the anode of the photocell is represented below:

$$I_2 + I^- \leftrightarrow I_3^-$$
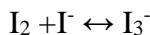
The reaction at the counter electrode is a reduction of tri- iodide ion to iodide is as shown:

$$I_{3^-} + 2e^- \rightarrow 3I^-$$
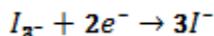
This stops the accumulation of holes which could cause recombination with electrons from the conduction band. Maximum output voltage equals to the difference between the redox potential of the mediator and the Fermi level of the semiconductor. Therefore, the DSSC can produce electricity from sunlight without going through any permanent physical and chemical change [18].The A.I of the dye cocktail of *C.acuminata*, *L.arboreus* and *B.spectabilis* was determined with Genesys 10S V1.200 model (2L7J355002) in 2014, this spectrograph was analysed with the spectrograph obtained in 2015. Figure 6a shows A.I of *C.acuminata* without electrolyte, it has a peak value of 4.0 within 200 nm to 900 nm wavelength in February, 2014. By January, 2015 (figure 6b) *C.acuminata* A.I had reduced to a peak value of 2.320. The series of hops were absent, indicating higher degree of stability for wavelength range of 500 nm to 800nm. Several –OH ligands have evaporated, *C.acuminata* is more concentrated. Figure 2a shows *C.acuminata* with three electrolytes, it had 5 mA, 9 mA and 3 mA with KCl, $HgCl_2$ and KBr respectively. KBr electrolyte did not give the desired effect; to boost the production of photocurrent. $HgCl_2$ increased photocurrent by 125% while, KCl's increase was 25% under AM 1.5.

(a)   *(b)*
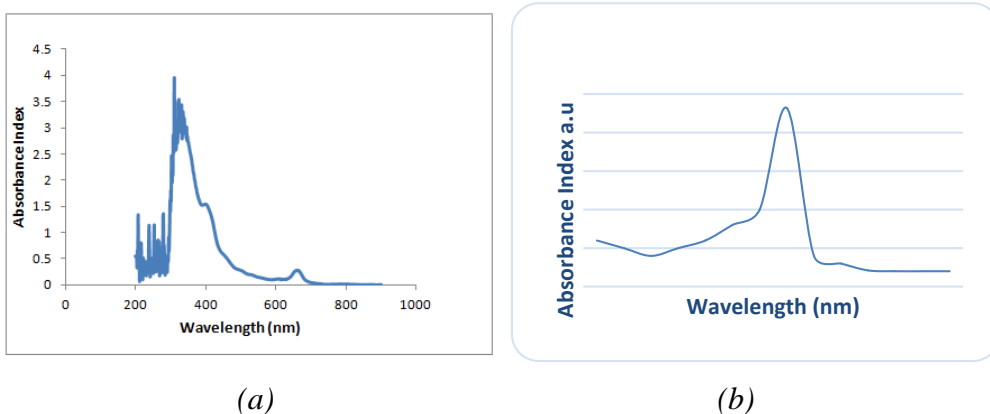
Figure 6. A.I of C.acuminata. a) In 2014 b) by 2015

Figure 7a features pure *L.arboreus* with A.I of about 2.0, when a cocktail of *L.arboreus* with *C.acuminata* and *B.spectabilis*, the drop in value of A.I could be attributed to unfavourable inter-dye interactions, dye degeneracy or a measure of both conditions[19].

(a)   (b)
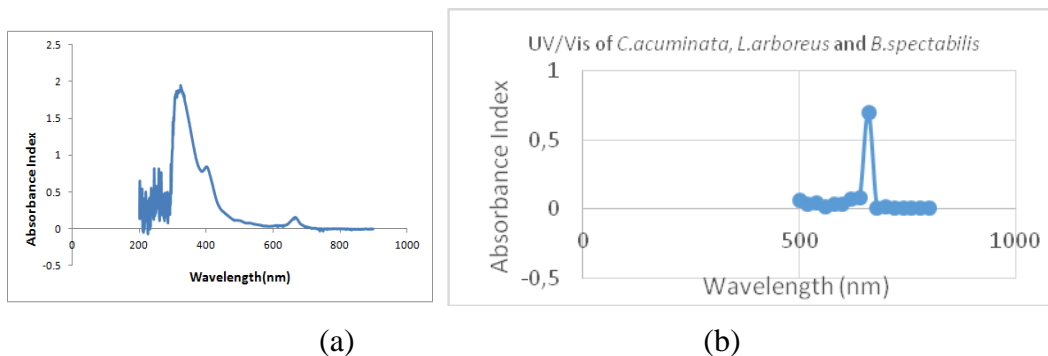
Figure 7.a) A.I of L.arboreus b) C.acuminata, B.spectabilis and L.arboreus dye (February 2014)

B.spectabilis has A.I of 1.6 (figure 8a), when mixed in cocktail with *C.acuminata* and *B.spectabilis* another A.I drop occurs to 0.520 affirming an unfavourable interaction between the three dyes[19].

(a)   (b)
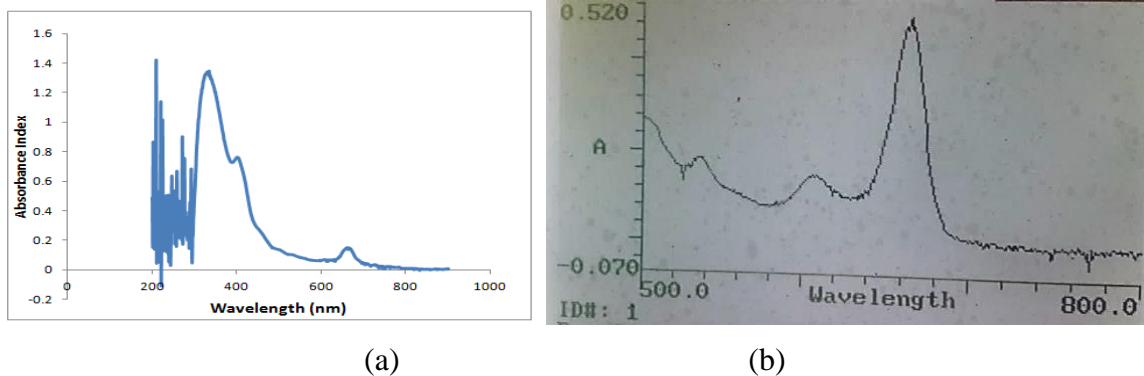
Figure 8.a) A.I of B.spectabilis b) C.acuminata, B.spectabilis and L.arboreus dye (January 2015)

Figure 7b shows a cocktail of *C.acuminata* and *B.spectabilis* in February, 2014 with no electrolyte. It is characterized by several short jumps or 'hops' from 200 nm to 300 nm, the highest A.I is at 1.4. Dye cocktail of *C.acuminata, B.spectabilis and L.arboreus dye* (figure 8b) also has the period of instability or hops, electron liberation, transfer and combination or recombination with holes. The peak A.I is 2.0 for wavelength range 200 nm to 900 nm (compare with figure 5b) *C.acuminata* and *B.spectabilis* with different electrolytes under AM 1.5. The photocurrent values were 19 mA, 9 mA and 13 mA respectively with KCl, $HgCl_2$ and KBr respectively. All three electrolytes showed very promising yield. However, by January, 2015 the yield had reduced due to degeneracy [13].

Rate of Photo Voltage Decay in DSSC. Photo voltage decay is inversely proportional to the lifetime of photo electrons in DSSCs and this lifetime in turn is inversely proportional to rate of recombination[19].The photo-degradation efficiency ŋ was calculated by

$$\eta = \frac{A_0 - A_i}{A_0} \times 100\%$$

$\eta_{c.acuminata}$ = 80%, dye cocktail of the three dyes from the formula has a photo-degeneracy of 53.8%. This indicates rate of decomposition of $\eta_{cocktail} < \eta_{c.acuminata}$ although the A.I for parent dye was higher for both *L.arboreus* and *C.acuminata*.

Summary. Photo-degeneracy in DSSCs is a single type contrary to Si wafers that have two lifetime. Generation and recombination lifetimes (τ_g and τ_r respectively), the dual function is combined in DSSCs.

DSSCs should last at least twenty years without significant degradation when sensitized with suitable electrolytes. Standard aging test last for 1000 hours typically[20], equivalent to a year of outdoor application. In practice, real outdoor tests data for years is not readily available. It implies linear degradation though a safe assumption might not affect I / V parameters in the short reaction time due to presence of large dye molecules on the electrode.

Each of these molecules undergoes 91 million redox cycles in those twenty years under AM 1.5 and moderate temperature between 55^0C-60^0C [20]. In an ideal condition, electron injection and regeneration occur irreversibly. In any device however, a measure of degradation occurs since a temperature of 80^0C is easily attained on a sunny day, the stability intrinsically is insufficient and requires improvement.

Improved stability by reducing electrolyte's vapour pressure or amending the interface of TiO_2-dye are advances achieved with ionic liquids as electrode sensitizers. Initial efficiency of 8.1% has been demonstrated when this TiO_2 network is immersed with quasi- solid state electrolyte. It is subject to debate if the polymer matrix can withstand intense UV irradiation without degradation.

Acknowledgements

References

[1] B. O'Regan and M. Gratzel, Nature (London) 353, 737 (1991).

[2] M. Gratzel, Nature (London) 414, 338 (2001).

[3] M. Durr, A. Bamedi, A. Yasuda, and G. Nelles, Appl. Phys. Lett. 84, 3397 (2004).

[4] W. U. Huynh, J. J. Dittmer and, A. P. Alivisatos, Science 295, 2425 (2002).

[5] M. K. Nazeeruddin, P. Pechy, T. Renouard, S. M. Zakeeruddin, R. Humphry-Baker, P. Compte, P. Liska, L. Cevey, E. Costa, V. Shklover, L. Spiccia, G. B. Deacon, C. A. Bignozzi, and M. Gratzel, J.Am. Chem. Soc. 123, 1613 (2001).

[6] D. Gebeyehu, C. J. Brabec, and N. S. Saiciftci, Thin Solid Films 403, 271 (2002).

[7] K. Keis, E. Magnusson, H. Lindstrom, S. E. Lindquist, and A. Hagfeldt, Sol. Energy Mater. Sol. Cells 73, 51 (2002).

[8] Z. S. Wang, C.H. Huang, Y.Y. Huang, Y.J. Hou, P.H. Xie, B.W. Zhang, and H.M. Cheng. Chem. Mater. 13, 678 (2001).

[9] J. Xia, N. Masaki, K. Jiang, S. Yanagida, Chem. Commun. 138 (2007).

[10] B. Peng, G. Jungmann, C. Jäger, D. Haarer, H.W. Schmidt, M. Thelakkat, Coord. Chem.Rev. 248, 1479 (2004).

[11] K. Zhu, E. A. Schiff, N. -G. Park, J. V. D. Lagemaat, A. J. Frank, Appl. Phys. Lett. 80, 685, (2002).

[12] A. Zaban, M. Greenshtein, J. Bisquetr, Chem. Phys. Chem 4, 859 (2003).

[13] A. Hagfeldt, M. Grätzel, Chem, Rev. 95, 49 (1995).

[14] A. Kumar, P. G. Santangelo, N. S. Lewis, J. Phys. Chem. 96, 834 (1992).

[15] D.K. Schroder, ''Surface Voltage and Surface Photovoltage: history, theory and applications'', Meas. Sci. technol. 12, (2001), R 16 – R 31.

[16] L. Peter, ''Infrared and Raman Characteristic Group Frequencies: Tables and Charts'', 18 (2011).

[17] I. Reiss, ''what does a voltmeter measure?'' Solid State Ionics, 95, 325, 1197.

[18] D. Chattopadhyay, ''Electronics (Fundamentals and Applications)''.

[19] B. Park, Q. Shen, Y. Ogomi, S.S. Pandey, T. Toyoda, S. Hayase, ECS Journal of Solid State Science and Technology. 2, 1 Q6 - Q11 (2013).

[20] J. Vlachopoulos, Particle Coalescence (sintering) in Polymer Processing and Beyond, PPS (2014).